NANO LETTERS
Cite This: Nano Lett. XXXX, XXX, XXX−XXX
Letter
pubs.acs.org/NanoLett

PVDF/Palygorskite Nanowire Composite Electrolyte for 4 V Rechargeable Lithium Batteries with High Energy Density

Pengcheng Yao,[†] Bin Zhu,[†,‡] Haowei Zhai,[†] Xiangbiao Liao,[§] Yuxiang Zhu,[†] Weiheng Xu,[†] Qian Cheng,[†] Charles Jayyosi,[∥] Zheng Li,[⊥] Jia Zhu,[‡] Kristin M. Myers,[∥] Xi Chen,[§] and Yuan Yang*[,†]

[†]Program of Materials Science and Engineering, Department of Applied Physics and Applied Mathematics, Columbia University, New York, New York 10027, United States
[‡]College of Engineering and Applied Science, Nanjing University, Nanjing, 210093, People's Republic of China
[§]Department of Earth and Environmental Engineering, Columbia University, New York, New York 10027, United States
[∥]Department of Mechanical Engineering, Columbia University, New York, New York 10027, United States
[⊥]Jiangsu Qingtao Energy S&T Co., Ltd, Huai-an, 211700, People's Republic of China

Supporting Information

ABSTRACT: Solid electrolytes are crucial for the development of solid state batteries. Among different types of solid electrolytes, poly(ethylene oxide) (PEO)-based polymer electrolytes have attracted extensive attention owing to their excellent flexibility and easiness for processing. However, their relatively low ionic conductivities and electrochemical instability above 4 V limit their applications in batteries with high energy density. Herein, we prepared poly(vinylidene fluoride) (PVDF) polymer electrolytes with an organic plasticizer, which possesses compatibility with 4 V cathode and high ionic conductivity (1.2×10^{-4} S/cm) at room temperature. We also revealed the importance of plasticizer content to the ionic conductivity. To address weak mechanical strength of the PVDF electrolyte with plasticizer, we introduced palygorskite ($(Mg,Al)_2Si_4O_{10}(OH)$) nanowires as a new ceramic filler to form composite solid electrolytes (CPE), which greatly enhances both stiffness and toughness of PVDF-based polymer electrolyte. With 5 wt % of palygorskite nanowires, not only does the elastic modulus of PVDF CPE increase from 9.0 to 96 MPa but also its yield stress is enhanced by 200%. Moreover, numerical modeling uncovers that the strong nanowire−polymer interaction and cross-linking network of nanowires are responsible for such significant enhancement in mechanically robustness. The addition of 5% palygorskite nanowires also enhances transference number of Li^+ from 0.21 to 0.54 due to interaction between palygorskite and ClO_4^- ions. We further demonstrate full cells based on $Li(Ni_{1/3}Mn_{1/3}Co_{1/3})O_2$ (NMC111) cathode, PVDF/palygorskite CPE, and lithium anode, which can be cycled over 200 times at 0.3 C, with 97% capacity retention. Moreover, the PVDF matrix is much less flammable than PEO electrolytes. Our work illustrates that the PVDF/palygorskite CPE is a promising electrolyte for solid state batteries.

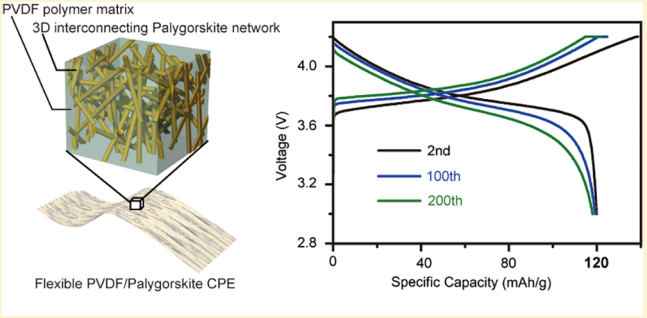

KEYWORDS: *Solid state battery, palygorskite, nanowire, PVDF, energy storage*

Solid-state lithium batteries have been intensively pursued as promising solutions to safety issues in Li-ion batteries with organic liquid electrolyte, such as leakage, flammability, and unstable solid-electrolyte interface (SEI) formation.[1−9] Solid electrolyte is critical to the successful development of solid state lithium batteries.[10−16] As an important class of solid electrolyte, polymer electrolytes, such as poly(ethylene oxide) (PEO), have attracted extensive attention due to their decent flexibility and facile processing compared with inorganic ceramic electrolytes.[17−19] However, the PEO-based polymer electrolytes (SPEs) usually show low ionic conductivity ($\sim 10^{-6}$ to 10^{-7} S/cm) with a low cation transference number (0.19 for $LiPF_6$) at room temperature,[18] severely restricting their practical applications.[20] Tremendous efforts have been made to increase the ionic conductivity of PEO-based electrolytes, such as cross-linking,[21] introducing ceramic fillers to form composite polymer electrolytes (CPEs),[22−27] and adding plasticizers.[28] Besides low conductivities, PEO tends to be oxidized above 4 V versus Li/Li^+, making it difficult to be paired with NMC materials and limiting energy density of the full cell. Therefore, developing polymer electrolyte stable with 4 V NMC cathodes and further enhancing their ionic conductivities are critical to practical applications of solid

Received: April 9, 2018
Revised: August 15, 2018
Published: August 31, 2018

DOI: 10.1021/acs.nanolett.8b01421
Nano Lett. XXXX, XXX, XXX−XXX

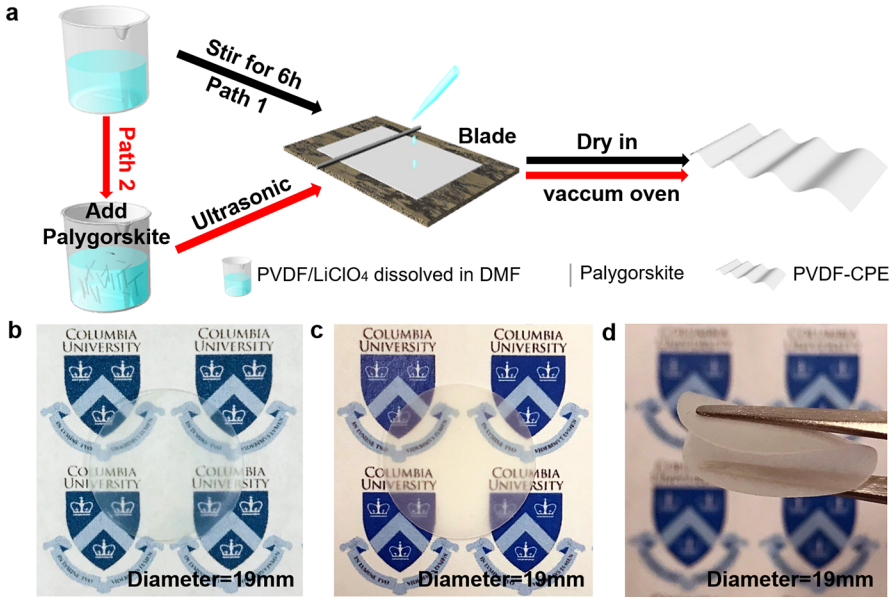

Figure 1. (a) A Schematic diagram of the synthesis of PVDF-based polymer electrolytes and PVDF/palygorskite nanowires/CPE. (b–d) (b) PVDF polymer electrolyte membrane and (c) PVDF/palygorskite CPE membrane dried at 60 °C in vacuum chamber for 24 h. (d) Bent PVDF/palygorskite CPE showing excellent flexibility.

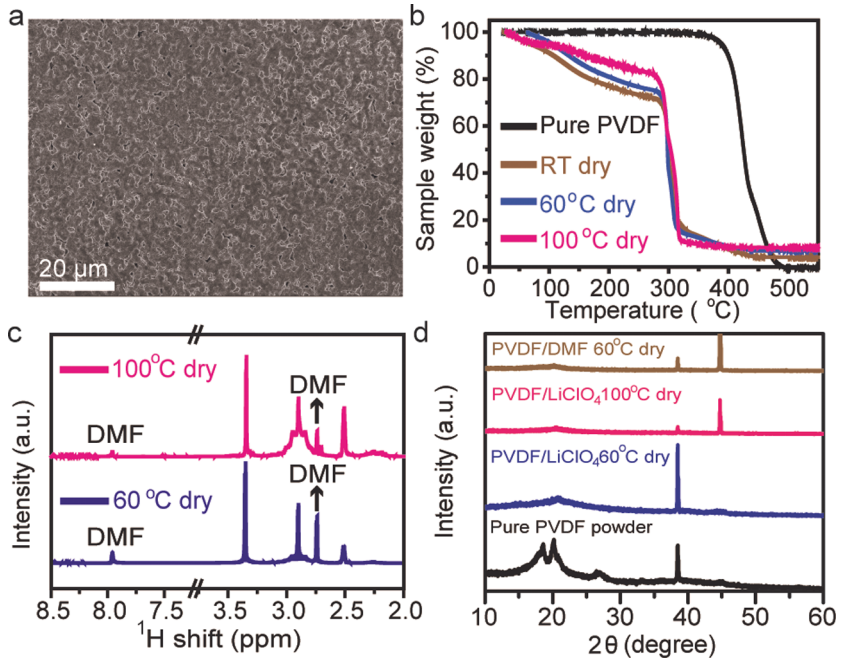

Figure 2. (a) SEM image of PVDF electrolyte vacuum-dried at 60 °C. (b) TGA curves of PVDF electrolyte under different temperatures in vacuum drying. (c) ^{1}H NMR spectra of 60 and 100 °C vacuum-dried PVDF-based polymer electrolytes. (d) XRD patterns of PVDF powder, PVDF electrolyte vacuum-dried at 60 °C, PVDF electrolyte vacuum-dried at 100 °C and PVDF/DMF vacuum-dried at 60 °C. The two peaks at 38.5° and 44.8° belongs to the aluminum substrate.

state lithium batteries. However, only occasional study on polymer electrolyte-based 4 V batteries is reported.[29]

Recently, poly(vinylidene fluoride) (PVDF) based polymer electrolytes attracted much attention due to their non-flammability, easy processing, wide electrochemical window and high ionic conductivity (~10^{-4} S/cm).[24,30] In investigating the underlying transport mechanism in PVDF electrolytes, we found that the quantity of dimethylformamide (DMF), which served as both solvent and plasticizer, played a significant role in ionic conductivity. On the basis of our results, when DMF remained at 20 wt % of the PVDF-based polymer gel electrolyte, its ionic conductivity became higher than 1 × 10^{-4} S/cm. However, a larger amount of DMF plasticizer may soften the composite electrolyte and make it vulnerable to dendrite penetration.

To solve this issue, we demonstrate that ceramic nanowire fillers are excellent candidates to enhance mechanical strength. As a demonstration, we show that PVDF CPEs with randomly dispersed and interconnecting palygorskite nanowires exhibit both high ionic conductivity and significantly enhanced

DOI: 10.1021/acs.nanolett.8b01421
Nano Lett. XXXX, XXX, XXX−XXX

mechanical properties. Palygorskite, a kind of magnesium aluminum silicate mineral ($(Mg,Al)_2Si_4O_{10}(OH)$), has been widely used as industrial floor absorbents, agricultural carriers, and environmental absorbents because of its open structure.[31,32] With one-dimensional fiber structure (~50 nm in diameter and ~1 μm in length), it can easily form an interconnected network even at low concentration to provide excellent mechanical property. When added as fillers in the PVDF-based polymer electrolytes, it largely enhances both the stiffness and toughnesss of the membrane. The mechanical robustness allows suppression of lithium dendrite and improves cycling stability. The addition of 5 wt % palygorskite nanowires also enhances transference number of Li^+ from 0.21 to 0.54 as a result of interaction between the nanowires and ClO_4^- anions. With such high-performance PVDF CPEs, a solid state lithium battery of $Li(Ni_{1/3}Mn_{1/3}Co_{1/3})O_2$ (NMC111)/PVDF/palygorskite CPE/Li presents a stable cycling over 200 times with 118.1 mAh/g discharge capacity retained. In addition to experiments, numerical calculations were also carried out, which further uncovers that nanowire–polymer interaction and interwire interactions are critical to the enhanced mechanical properties of samples with palygorskite nanowires added.

The free-standing PVDF-based polymer electrolytes and PVDF/palygorskite CPEs were prepared through a facile solution-casting method (Figure 1a). First, PVDF powders (Arkema Kynar 761), $LiClO_4$, and a certain amount of palygorskite nanowires were dissolved in DMF and stirred for 6 h at 50 °C (Figure S1a). Then the solution was cast on glass and vacuum-dried at different temperatures between 25 to 120 °C to obtain free-standing PVDF-based polymer electrolytes containing different amount of DMF. The film thickness is ~100 μm. When vacuum-dried below 60 °C, the polymer electrolyte membrane is highly transparent and flexible, as shown in Figure 1c,d. However, if vacuum-dried above 80 °C, it turns nontransparent and the color changes from white to pale yellow (Figure S1c,d). After adding palygorskite, the obtained PVDF CPEs are translucent with good flexibility (Figure 1d).

The PVDF-based polymer electrolytes dried at various temperatures were first characterized by scanning electron microscopy (SEM). As shown in Figure 2a, compact and flat films with PVDF microstructures are presented, which help improve ionic conductivity. To investigate the thermal stability of PVDF polymer electrolytes and evaluate the amount of DMF inside, thermogravimetric analysis (TGA) and nuclear magnetic resonance (NMR) were performed. As shown in TGA results (Figure 2b), apparent weight loss occurs in PVDF-based polymer electrolytes below 300 °C but not in pure PVDF. To understand the mechanism behind this, TGA tests were further performed in PVDF/$LiClO_4$ and PVDF/DMF binary membranes (Figure S2a). The $LiClO_4$-free PVDF/DMF membrane shows significant weight loss at 400 °C, similar to pure PVDF, but the DMF-free PVDF/$LiClO_4$ film shows remarkable weight loss at 300 °C similar to the polymer electrolyte. Therefore, the reduced thermal stability should be a result of $LiClO_4$, which is a well-known oxidant and accelerates the decomposition of PVDF. Nevertheless, stability up to 300 °C is still attractive for lithium batteries. To further determine the quality of DMF in different PVDF polymer electrolytes, ^{1}H NMR test was carried out. The two peaks for DMF are located at 2.7 and 8.0 ppm (Figure 2c). Quantitative analysis show that the amount of DMF left are 23.6, 6.3, and 3.3 wt % for sample vacuum-dried at 60, 80, and 100 °C, respectively (Table 1).

Table 1. Relationship between Vacuum Dried Temperature, DMF Content, and Ionic Conductivity

vacuum dried temperature (°C)	DMF content (wt %)	ionic conductivity (S/cm)
60	23.6	1.2×10^{-4}
80	6.3	2.0×10^{-6}
100	3.3	1.1×10^{-6}

To further understand the effect of DMF on PVDF-based polymer electrolytes compared with pure PVDF powders, X-ray diffraction (XRD) and Raman characterizations were also carried out. Although PVDF itself shows two small peaks at 18.5° and 20.1°, which corresponds to α-phase PVDF,[33,34] these two peaks do not exist in PVDF polymer electrolyte membrane indicating the amorphrization of PVDF. Although PVDF itself shows two small peaks at 18.5° and 20.1°, which corresponds to α-phase PVDF,[33,34] these two peaks do not exist in PVDF polymer electrolyte membrane. Furthermore, these two peaks also vanish both in PVDF/DMF and PVDF/$LiClO_4$ binary membrane, indicating that both the DMF plasticizer and $LiClO_4$ amorphorize the film (Figure 2d). The peak at 38.5° and 44.8° come from the aluminum substrate. The existence of DMF and $LiClO_4$ are also clearly shown in the Raman spectrum (Figure S2b), as indicated by peaks at 869, 1105, 1421, and 1443 cm^{-1} for DMF[35] and 935 cm^{-1} for $LiClO_4$.[36]

To understand the effect of DMF amount on PVDF polymer electrolyte conductivity, the ionic conductivities of PVDF polymer electrolytes at various temperatures were investigated by electrochemical impedance spectroscopy (EIS) measurements in a stainless steel/PVDF-based polymer electrolyte/stainless steel configuration. The corresponding Nyquist plots at room temperature are presented in Figure S3. Then ionic conductivities σ are calculated based on four samples at each drying temperature (Figure 3a). At room temperature, the ionic conductivity of PVDF polymer electrolyte vacuum-dried at 25 °C reaches 1.4×10^{-4} S/cm, which is similar to 1.2×10^{-4} S/cm for 60 °C sample, consistent with previous reports.[24] A sudden drop is observed between drying temperature of 70 and 80 °C, where conductivities decreases from 1.2×10^{-4} to 2.0×10^{-6} S/cm, and it further decreases to 1.1×10^{-6} S/cm for samples dried at 100 °C. This is consistent with the decreasing concentration of DMF in the electrolyte upon heating. The sudden drop between 70 and 80 °C indicates that DMF concentration decreases to a level lower than a critical threshold. The DMF concentration also affects the activation energy of ion transport. As shown in σ versus T plot in Figure 3b, the activation barriers are 0.39, 0.42, 0.64, and 0.63 eV for RT, 60, 80, and 100 °C dried samples. This indicates that high DMF content also reduces activation barrier to facilitate ion transport. These results indicates that DMF is critical to the ionic conductivity of such PVDF-based polymer electrolyte. At a weight content of 23.6%, the polymer electrolyte can be considered as a gel electrolyte or a hybrid solid/liquid electrolyte too.

To figure out how the DMF plasticizer affects electrochemical stability, cyclic voltammetry was performed at room temperature for PVDF polymer electrolyte samples dried at 60 °C. No obvious oxidation starts until 4.7 V versus Li/Li^+,

DOI: 10.1021/acs.nanolett.8b01421
Nano Lett. XXXX, XXX, XXX–XXX

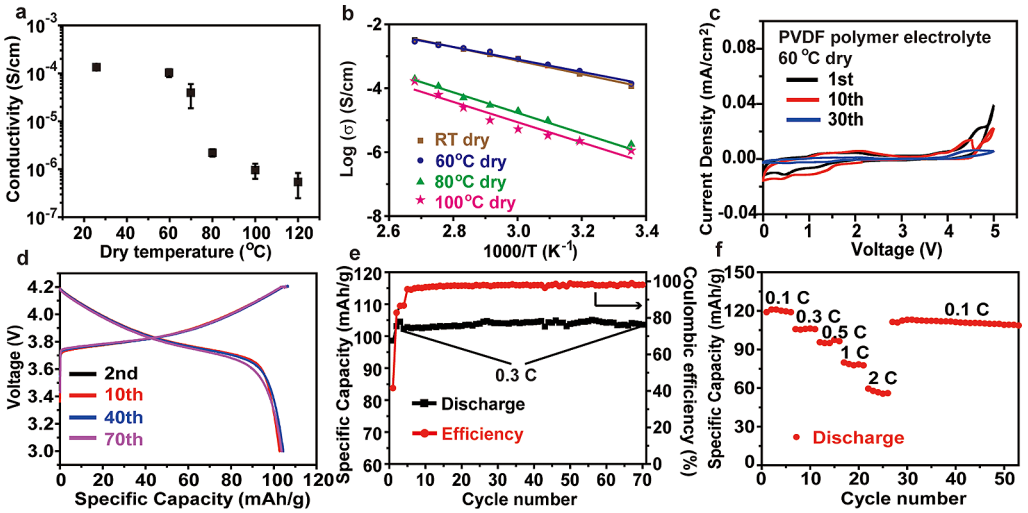

Figure 3. (a) The conductivities of PVDF polymer electrolytes as a function of vacuum-dried temperatures. (b) Arrhenius plots of the PVDF based polymer electrolytes. (c) Cycle voltammetry curve of PVDF polymer electrolyte dried at 60 °C in vacuum. (d) Typical charge−discharge curves of NMC 111/PVDF/Li cells between 4.2 and 3.0 V at 0.3 C. (e) Cycle performance of a NMC 111/PVDF polymer electrolyte/Li cell at 0.3 C (1 C = 150 mA/g). (f) Power capability of such NMC111/PVDF/Li cell between 0.1 and 2 C rates.

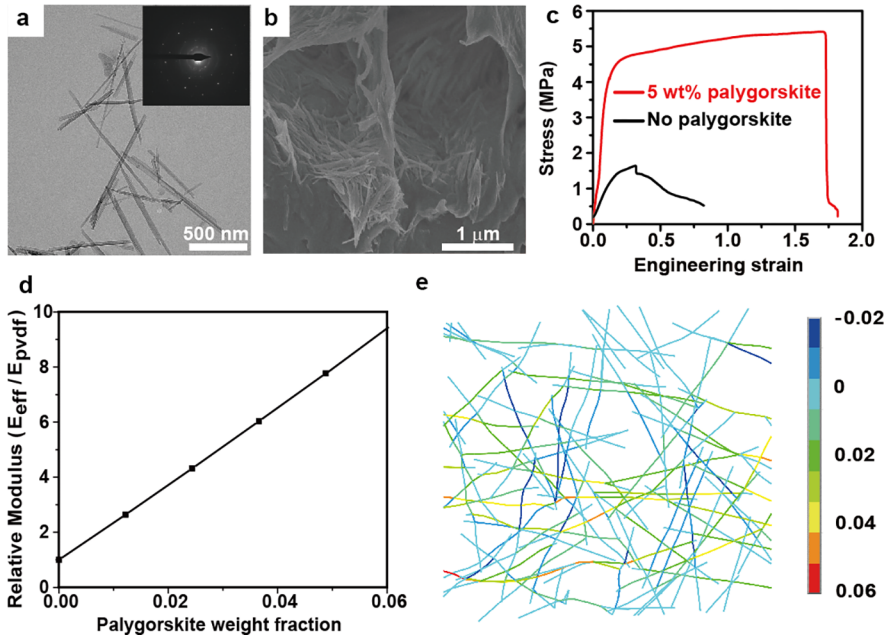

Figure 4. (a) A TEM image of paylgorskite nanowires and corresponding electron diffraction pattern. (b) Cross-sectional SEM image of PVDF/palygorskite-CPE, showing that palygorskite nanowires blended into the PVDF matrix. (c) Stress−strain relations of different PVDF-based membranes under uniaxial tension at strain rate of 0.001/s. (d) Effective Young's modulus of composite membrane with randomly distributed nanowire fillers as a function of weight fraction. (e) Axial strain contour of the deformed nanowire network at an average tensile strain of 5%.

indicating that the PVDF/$LiClO_4$ membrane can be stable with 4 V NMC cathodes (Figure 3c). To further evaluate their electrochemical performance, cells with $Li(Ni_{1/3}Mn_{1/3}Co_{1/3})O_2$ cathode (NMC 111), Li metal anode, and PVDF polymer electrolyte dried at 60 °C were assembled. The average thickness of PVDF/electrolyte is 100 μm. The active material is around 1.6 mg/cm^2. All the battery tests were operated at 25 °C.The PVDF polymer electrolyte-cells were cycled between 4.2 and 3.0 V at 0.1 C (15 mA/g) for three cycles first, followed by 0.3 C for 70 cycles. In charging, a constant voltage step with a cutoff of C/20 is added at 4.2 V (Figure 3d). The discharge capacity slightly increases from 98.6 mA/g in cycle 1 to a peak value of 105.1 mA/g in cycle 58 and remains at 103.6 mAh/g at cycle 70 (Figure 3e). The specific capacity is also close to results in liquid electrolyte, which is ∼125 mAh/g between 3.0 and 4.2 V (Figure S5c,d). The power capability test shows that the specific capacity remains at 106.2, 97.4, 79.8, and 59.5 mAh/g at 0.2, 0.5, 1, and 2 C, respectively, which indicates reasonable rate performance of the PVDF polymer electrolyte cell.

Although DMF helps to increase ionic conductivity, the mechanical robustness of PVDF/$LiClO_4$ membrane is seriously weakened (Figure 4c), which will comprise its capability against lithium dendrite and deteriorate battery safety.[37] To solve this issue, palygorskite ($(Mg,Al)_2Si_4O_{10}(OH)$) nanowires are added into the solid

DOI: 10.1021/acs.nanolett.8b01421
Nano Lett. XXXX, XXX, XXX−XXX

electrolyte membranes as reinforcing elements to improve the mechanical properties. There are two reasons to choose this material. First, its nanowire shape can help form an interconnected and mechanically strong network.[38,39] Second, palygorskite is a natural product with ultralow cost, much less than that to synthesize SiO_2,[40] Al_2O_3,[41] or ceramic electrolyte (e.g., LLZO[42]) nanowires. TEM characterizations show that palygorskite nanowires have a diameter of ∼50 nm and a length of ∼1 μm (Figure 4a). It is also crystalline based on electron diffraction data (inset in Figure 4a). To prepare PVDF/palygorskite CPEs, palygorskite nanowires were added into DMF/PVDF solution with target weight percentage. The cross-section SEM picture of palygorskite-modified membrane in Figure 4b further illustrates that palygorskite nanowires blend into the PVDF polymer matrix.

The enhancement in mechanical properties is demonstrated as the stress−strain responses of pure PVDF polymer electrolyte and PVDF/5 wt % palygorskite CPE at a constant tensile strain rate of 0.001/*s*, as shown in Figure 4c. Adding 5 wt % palygorskite nanowires to the PVDF polymer electrolyte not only significantly improves the Young's modulus from 9.0 to 96 MPa of membrane but also increases the yield stress by 200% (4.7 MPa versus 1.5 MPa). Although this value is much less than the threshold proposed by Newman,[43] (shear modulus of 6.8 GPa), previous studies have shown that even lower Young's modulus of electrolyte can help suppress the dendrite growth to realize long-term cycling stability.[10,44,45] To unveil the connection between dendrite suppression and the addition of palygorskite nanowires, shorting time during lithium plating and SEM characterizations are carried out (Figure S6). When 0.3 mA/cm^2 is applied, the Li/Li cell with pure PVDF polymer electrolyte is shorted after only 3.8 h, which is equivalent to 1.14 mAh/cm^2. Meanwhile, the time for 3 wt % palygorskite/PVDF CPE and 5 wt % palygorskite/PVDF CPE are 26 and 36 h, respectively, corresponding to 7.8 and 10.8 mAh/cm^2, respectively. Moreover, the lithium surface with CPE is also much smoother than that without palygorskite addition (Figure S6f). This indicates that the addition of palygorskite nanowires in such CPE can suppress the growth of lithium dendrites. In our own full cell cycling, we also find that the addition of palygorskite nanowires enhances cycling life, as discussed below, but it should be noted that further investigations should be carried out to fully understand its capability to suppress dendrite, especially at high currents.

Mechanical-wise, it is impressive that adding such a small amount of palygorskite can greatly improve the mechanical properties. To unveil the mechanisms behind, both theoretical and numerical analyses were performed. The enhanced stiffness of this composite can be mainly attributed to the matrix−nanowires interaction. In Figure 4d, analysis based on the Mori-Tanaka's theory indicates that with 5 wt % palygorskite the effective modulus E_{eff} can reach eight times that of pure PVDF matrix,[46] slightly smaller than measured results of 10.7 times. The deviation is possibly due to the nanowire−nanowire interaction in a cross-linked network through nanowelding junctions, van der Waal interaction, and chemical bonds. To verify the effect of such internanowire interaction, Monte Carlo and finite element simulations were carried out to generate a network of 5 wt % randomly distributed nanowires, and nanowire deformation with the network externally stretched is calculated, as shown in Figure 4e. A significant portion of axial strain is undertaken by wire−wire junction, which indicates enhanced stiffness by forming wire−wire junctions as hinges. Therefore, we attribute both the nanowire−polymer interaction and the internanowire connections to be responsible for the increased stiffness of modified PVDF polymer electrolyte membrane. Additionally, the composite electrolyte shows significantly increased fracture strain of 180%, which is twice that of pure PVDF polymer electrolyte membrane (90%) (Figure 4c). This toughening effect should be due to strong interfacial adhesion between nanowires and PVDF matrix,[47] resisting nanowire pull-out when composite fracturing. Therefore, the additives of palygorskite nanowires allow the PVDF-based membrane to be mechanically robust, underpinning safety of solid electrolyte.

To further evaluate the effect of palygorskite nanowires on PVDF-based CPEs, the ionic conductivities of PVDF CPEs with different weight percentages of paylgorskite nanowires were investigated. All samples are dried in vacuum oven at 60 °C for 24 h, and four samples were tested for each weight percentage. The ionic conductivities of 1, 3, and 5 wt % PVDF/palygorskite CPEs reach 1.4×10^{-4}, 1.7×10^{-4}, and 8.3×10^{-5} S/cm, respectively. It is likely that due to the high aspect ratio of nanowires, only 1−3 wt % is enough to form a network and facilitate ionic transport, while adding more will block ion transport and thus reduce ionic conductivity. The corresponding activation barriers are 0.46, 0.32, and 0.36 eV, respectively (Figure S4a), similar to samples without palygorskite nanowires (Figure 3b). Also, the lithium ion transference number (t_{Li+}) of PVDF/palygorskite and PVDF polymer electrolytes were measured through potentiostatic polarization (PP) method (Figure S7).[48] The calculated t_{Li+} for the PVDF/5 wt % palygorskite CPE, PVDF/3 wt % palygorskite CPE, and PVDF polymer electrolytes are 0.54, 0.31 and 0.21, respectively. The enhanced t_{Li+} is likely due to two reasons. First, with the addition of inorganic fillers the local chains of polymer can be relaxed and the segment motion is promoted under the interaction of inorganic fillers and polymer chains; as a result, the mobility of Li ions and t_{Li+} can be enhanced.[30] Apart from stabilizing the amorphous state of the polymer, the exposed metal cations on the surface of palygorskite ceramic nanowires also interacts with ClO_4^- through Lewis acid−base interactions.[49] So, there may be interaction between the palygorskite and anions in the lithium salt which immobilize anion and enhance transference number. This assumption is confirmed through FTIR test (Figure S8). The ClO_4^- peaks at 1663 cm^{-1} in PVDF polymer electrolyte shift to 1652 cm^{-1} in PVDF/palygorskite CPEs. The shape of the peak at 3559 cm^{-1} also changes. These shifts in FTIR can be attributed to the interaction between palygorskite nanowires and the ClO_4^- anion, which alters the vibration modes in ClO_4^-. Such interactions enhances dissociation of $LiClO_4$, traps ClO_4^- on nanowire surface, and thus increases transference number of Li^+. This has been observed in $Mg_2B_2O_5$[27] and $Li_7La_3Zr_2O_{12}$.[30]

To further examine the electrochemical stability of PVDF/palygorskite CPEs, cyclic voltammetry is carried out first, as shown in Figure S9. The cathodic current density at 0 V versus Li^+/Li is ∼1 μA/cm^2, much smaller than that in pure PVDF membrane (Figure 3c). Because palygorskite nanowire is a well-known absorbent for organic solvent,[32] they could trap DMF and reduce its reduction rate. Furthermore, full cell tests were performed with 5 wt % palygorskite nanowire fillers, and steady cycling is achieved, too (Figure 5a). The cycling protocol is the same as pure PVDF polymer electrolyte, 0.1 C

DOI: 10.1021/acs.nanolett.8b01421
Nano Lett. XXXX, XXX, XXX−XXX

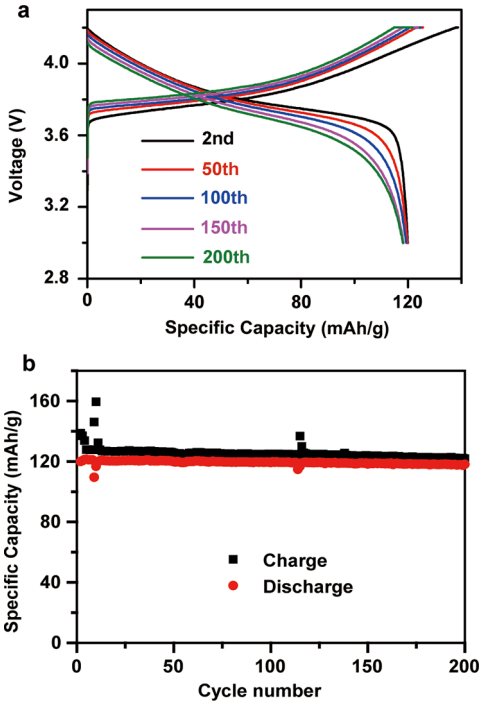

Figure 5. (a) Voltage profile and (b) cycling performance of NMC|PVDF/5 wt % palygorskite CPE|Li cell. (1 C = 150 mA/g).

for three cycles, followed by 0.3 C between 4.2 and 3.0 V. At 0.3 C, the discharge capacity rises from 117.6 to 121.4 mAh/g in the first 5 cycles and retains at 118.1 mAh/g after 200 cycles at 0.3 C. (Figure 5b), which shows that PVDF/palygorskite CPEs work steadily in the cell. Similarly, NMC/Li cells with 1 and 3 wt % of palygorskite nanowires were also tested for comparison. While similar cycling stability can be obtained, we noticed that cells with no or a lower amount of palygorskite nanowires tend to have microshorting in a smaller number of cycles (e.g., ~90 cycles for 1 wt % and ~130 cycles for 3 wt %, Figure S5b). Meanwhile, 5 wt % sample shows stability over 200 cycles and ongoing. This also indicates that the addition of palygorskite nanowires in such CPE can suppress the penetration of lithium dendrite so that a longer cycle life can be achieved. However, the performance of lithium/lithium symmetric cells (Figure S4b,c) is not as good as the NMC 111|PVDF/palygorskite CPE|Li cells. A possible reason is that in lithium/lithium symmetric cells, lithium metal is oxidized first at one electrode, which results in fresh new lithium metal surface that directly exposes to DMF, that may accelerate the degradation of cycling performance. This was also observed in past literature.[24] In the future, we will modify lithium surface (e.g., passivation layer[50,51]), or replace DMF with more stable plasticizers, to address this issue.

Besides electrochemical performance, safety and nonflammability are also crucial to evaluate solid electrolytes. To prove the safety of PVDF-based solid electrolytes, nailing test was conducted. In the experiment, a pouch cell with PVDF CPE, NMC cathode and lithium anode was assembled, embedded with thermocouple to detect the real-time temperature changes. The cell was precharged to 4.0 V and a stainless steel syringe needle was used to penetrate the pouch to mimic short circuit (Figure 6a). As shown in Figure 6c, after puncturing the cell voltage decreased to 17 mV, but there is no significant increase in cell temperature showing limited safety

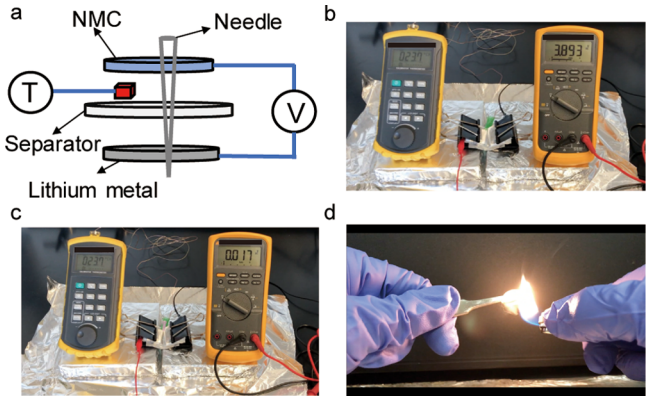

Figure 6. (a) The schematic diagram of the nailing test. (b) NMC/PVDF−palygorskite CPE/Li pouch cell before (b) and after (c) puncture. (d) Ignition test of PVDF film vacuum-dried at 60 °C. The film does not catch fire when ignited.

hazards. Besides puncturing, PVDF film vacuum-dried at 60 °C is also not ignitable under fire, as shown in Figure 6d and Video S2. In contrast, pure PEO electrolyte can be easily ignited with fire. Such significant contrast further demonstrates the enhanced safety of PVDF-based solid electrolyte.

In summary, we successfully prepared flexible PVDF/palygorskite composite electrolyte membranes using a simple one-step solution-casting method. DMF serves as both solvent and plasticizer. When vacuum-dried at 60 °C, the plasticized PVDF membrane reaches a high conductivity of 1.2×10^{-4} S/cm. To address the softness issue of PVDF membrane with DMF plasticizer, palygorskite nanowires are uniformly dispersed in the CPE to form an interconnecting network, which greatly enhanced its mechanical properties. When only 5% palygorskite nanowires are added, the elastic modulus of PVDF CPE increases from 9.0 to 96 MPa, together with three times the enhancement in yield stress (4.7 MPa versus 1.5 MPa). Besides greatly improved mechanical properties, the PVDF/palygorskite CPE also shows excellent electrochemical performance at room temperature. An NMC 111|PVDF/palygorskite CPE|Li cells shows high capacity of 121.4 mAh/g at C/3 and steady cycling over 200 cycles. The specific capacity decays only 0.02% per cycle and remains at 118.1 mAh/g after 200 cycles at room temperature. All these results show that the PVDF/palygorskite CPE have great potential to satisfy the high energy density and safety requirements for next generation solid-state lithium batteries.

■ ASSOCIATED CONTENT

Supporting Information

The Supporting Information is available free of charge on the ACS Publications website at DOI: 10.1021/acs.nanolett.8b01421.

Preparation of polymer and composite electrolyte, material characterization, EIS for PVDF polymer electrolytes and CPE membranes, full cell test of PVDF/palygorskite CPE cells, shorting time experiment and SEM characterizations, measurement of lithium ion transference number (t_{Li+}) of PVDF based polymer electrolytes, cyclic voltammetry of 5 wt % palygorskite/PVDF CPE, mechanical tests for the composite films, calculation of effective Young's modulus of nanowire/PVDF polymer electrolyte composites, Monte Carlo simulations of 2D networks, finite element method

DOI: 10.1021/acs.nanolett.8b01421
Nano Lett. XXXX, XXX, XXX−XXX

simulation of 2D nanowire networks, additional figures (PDF)
Additional video (AVI)
Video PVDF film vacuum-dried at 60 °C not igniting under fire (AVI)

AUTHOR INFORMATION

Corresponding Author

*E-mail: yy2664@columbia.edu.

ORCID

Pengcheng Yao: 0000-0002-4022-7491
Haowei Zhai: 0000-0002-7030-3563
Xiangbiao Liao: 0000-0001-8214-454X
Qian Cheng: 0000-0001-5510-2977
Jia Zhu: 0000-0002-2871-4369
Yuan Yang: 0000-0003-0264-2640

Author Contributions

P.Y., B.Z., H.Z., and X.L. contributed equally to this paper.

Notes

The authors declare no competing financial interest.

ACKNOWLEDGMENTS

Y.Y. acknowledges support from startup funding by Columbia University. This work is supported by the NSF MRSEC program through Columbia in the Center for Precision Assembly of Superstratic and Superatomic Solids (DMR-1420634). B.Z. and X.L. acknowledge support from the China Scholarship Council (CSC) graduate scholarship.

REFERENCES

(1) Armand, M.; Endres, F.; MacFarlane, D. R.; Ohno, H.; Scrosati, B. *Nat. Mater.* **2009**, *8* (8), 621−629.
(2) Xu, K. *Chem. Rev.* **2004**, *104* (10), 4303−4417.
(3) Goodenough, J. B.; Park, K. S. *J. Am. Chem. Soc.* **2013**, *135* (4), 1167−1176.
(4) Lin, D. C.; Liu, Y. Y.; Cui, Y. *Nat. Nanotechnol.* **2017**, *12* (3), 194−206.
(5) Cheng, X. B.; Peng, H. J.; Huang, J. Q.; Zhang, R.; Zhao, C. Z.; Zhang, Q. *ACS Nano* **2015**, *9* (6), 6373−6382.
(6) Cheng, X. B.; Yan, C.; Chen, X.; Guan, C.; Huang, J. Q.; Peng, H. J.; Zhang, R.; Yang, S. T.; Zhang, Q. *Chem.* **2017**, *2* (2), 258−270.
(7) Cheng, X. B.; Zhang, Q. *J. Mater. Chem. A* **2015**, *3* (14), 7207−7209.
(8) Rettenwander, D.; Redhammer, G.; Preishuber-Pflugl, F.; Cheng, L.; Miara, L.; Wagner, R.; Welzl, A.; Suard, E.; Doeff, M. M.; Wilkening, M.; Fleig, J.; Amthauer, G. *Chem. Mater.* **2016**, *28* (7), 2384−2392.
(9) Yang, C. Y.; Ji, X.; Fan, X. L.; Gao, T.; Suo, L. M.; Wang, F.; Sun, W.; Chen, J.; Chen, L.; Han, F. D.; Miao, L.; Xu, K.; Gerasopoulos, K.; Wang, C. S. *Adv. Mater.* **2017**, *29* (44), 1701972.
(10) Zhai, H. W.; Xu, P. Y.; Ning, M. Q.; Cheng, Q.; Mandal, J.; Yang, Y. *Nano Lett.* **2017**, *17* (5), 3182−3187.
(11) Fu, K.; Gong, Y.; Dai, J.; Gong, A.; Han, X.; Yao, Y.; Wang, C.; Wang, Y.; Chen, Y.; Yan, C.; Li, Y.; Wachsman, E. D.; Hu, L. *Proc. Natl. Acad. Sci. U. S. A.* **2016**, *113* (26), 7094−7099.
(12) Tao, X. Y.; Liu, Y. Y.; Liu, W.; Zhou, G. M.; Zhao, J.; Lin, D. C.; Zu, C. X.; Sheng, O.; Zhang, W. K.; Lee, H. W.; Cui, Y. *Nano Lett.* **2017**, *17* (5), 2967−2972.
(13) Zhao, C. Z.; Zhang, X. Q.; Cheng, X. B.; Zhang, R.; Xu, R.; Chen, P. Y.; Peng, H. J.; Huang, J. Q.; Zhang, Q. *Proc. Natl. Acad. Sci. U. S. A.* **2017**, *114* (42), 11069−11074.
(14) Cheng, L.; Chen, W.; Kunz, M.; Persson, K.; Tamura, N.; Chen, G. Y.; Doeff, M. *ACS Appl. Mater. Interfaces* **2015**, *7* (3), 2073−2081.
(15) Cheng, L.; Hou, H. M.; Lux, S.; Kostecki, R.; Davis, R.; Zorba, V.; Mehta, A.; Doeff, M. *J. Electroceram.* **2017**, *38* (2−4), 168−175.
(16) Yao, X. Y.; Huang, N.; Han, F. D.; Zhang, Q.; Wan, H. L.; Mwizerwa, J. P.; Wang, C. S.; Xu, X. X. *Adv. Energy Mater.* **2017**, *7* (17), 1602923.
(17) Lin, D. C.; Liu, W.; Liu, Y. Y.; Lee, H. R.; Hsu, P. C.; Liu, K.; Cui, Y. *Nano Lett.* **2016**, *16* (1), 459−465.
(18) Xue, Z. G.; He, D.; Xie, X. L. *J. Mater. Chem. A* **2015**, *3* (38), 19218−19253.
(19) Zhang, J. X.; Zhao, N.; Zhang, M.; Li, Y. Q.; Chu, P. K.; Guo, X. X.; Di, Z. F.; Wang, X.; Li, H. *Nano Energy* **2016**, *28*, 447−454.
(20) Liu, W.; Song, M. S.; Kong, B.; Cui, Y. *Adv. Mater.* **2017**, *29* (1), 1603436.
(21) Fu, K. K.; Gong, Y. H.; Liu, B. Y.; Zhu, Y. Z.; Xu, S. M.; Yao, Y. G.; Luo, W.; Wang, C. W.; Lacey, S. D.; Dai, J. Q.; Chen, Y. N.; Mo, Y. F.; Wachsman, E.; Hu, L. B. *Science Advances* **2017**, *3* (4), 1601659.
(22) Liu, W.; Lin, D. C.; Sun, J.; Zhou, G. M.; Cui, Y. *ACS Nano* **2016**, *10* (12), 11407−11413.
(23) Liu, W.; Lee, S. W.; Lin, D. C.; Shi, F. F.; Wang, S.; Sendek, A. D.; Cui, Y. *Nature Energy* **2017**, *2* (5), 17035.
(24) Zhang, X.; Liu, T.; Zhang, S. F.; Huang, X.; Xu, B. Q.; Lin, Y. H.; Xu, B.; Li, L. L.; Nan, C. W.; Shen, Y. *J. Am. Chem. Soc.* **2017**, *139* (39), 13779−13785.
(25) Bae, J.; Li, Y.; Zhang, J.; Zhou, X.; Zhao, F.; Shi, Y.; Goodenough, J.; Yu, G. *Angew. Chem.* **2018**, *130*, 2025.
(26) Wang, C. S.; Zhang, X. W.; Appleby, A. J. *J. Electrochem. Soc.* **2005**, *152* (1), A205−A209.
(27) Sheng, O.; Jin, C.; Luo, J.; Yuan, H.; Huang, H.; Gan, Y.; Zhang, J.; Xia, Y.; Liang, C.; Zhang, W. *Nano Lett.* **2018**, *18*, 3104.
(28) Li, J. C.; Ma, C.; Chi, M. F.; Liang, C. D.; Dudney, N. J. *Adv. Energy Mater.* **2015**, DOI: 10.1002/aenm.201570018.
(29) Zhang, J. J.; Zang, X.; Wen, H. J.; Dong, T. T.; Chai, J. C.; Li, Y.; Chen, B. B.; Zhao, J. W.; Dong, S. M.; Ma, J.; Yue, L. P.; Liu, Z. H.; Guo, X. X.; Cui, G. L.; Chen, L. Q. *J. Mater. Chem. A* **2017**, *5* (10), 4940−4948.
(30) Zhang, W. Q.; Nie, J. H.; Li, F.; Wang, Z. L.; Sun, C. Q. *Nano Energy* **2018**, *45*, 413−419.
(31) Zuo, S. X.; Chen, J.; Liu, W. J.; Li, X. Z.; Kong, Y.; Yao, C.; Fu, Y. S. *Carbon* **2018**, *129*, 199−206.
(32) Murray, H. H. *Appl. Clay Sci.* **2000**, *17* (5−6), 207−221.
(33) Wang, J.; Li, H.; Liu, J.; Duan, Y.; Jiang, S.; Yan, S. *J. Am. Chem. Soc.* **2003**, *125* (6), 1496−1497.
(34) Gregorio, R. *J. Appl. Polym. Sci.* **2006**, *100* (4), 3272−3279.
(35) Kuzmin, A. N.; Pliss, A.; Lim, C.-K.; Heo, J.; Kim, S.; Rzhevskii, A.; Gu, B.; Yong, K.-T.; Wen, S.; Prasad, P. N. *Sci. Rep.* **2016**, *6*, 28483.
(36) Giorgini, M. G.; Futamatagawa, K.; Torii, H.; Musso, M.; Cerini, S. *J. Phys. Chem. Lett.* **2015**, *6* (16), 3296−3302.
(37) Bachman, J. C.; Muy, S.; Grimaud, A.; Chang, H. H.; Pour, N.; Lux, S. F.; Paschos, O.; Maglia, F.; Lupart, S.; Lamp, P.; Giordano, L.; Shao-Horn, Y. *Chem. Rev.* **2016**, *116* (1), 140−162.
(38) Chen, Y. L.; Pan, F.; Guo, Z. Y.; Liu, B.; Zhang, J. Y. *J. Mech. Phys. Solids* **2015**, *84*, 395−423.
(39) Pal, G.; Kumar, S. *Progress in Aerospace Sciences* **2016**, *80*, 33−58.
(40) Hessel, C. M.; Henderson, E. J.; Veinot, J. G. *Chem. Mater.* **2006**, *18* (26), 6139−6146.
(41) Ghosh, S.; Mashayekhi, H.; Bhowmik, P.; Xing, B. *Langmuir* **2010**, *26* (2), 873−879.
(42) Luo, W.; Gong, Y. H.; Zhu, Y. Z.; Li, Y. J.; Yao, Y. G.; Zhang, Y.; Fu, K.; Pastel, G.; Lin, C. F.; Mo, Y. F.; Wachsman, E. D.; Hu, L. B. *Adv. Mater.* **2017**, *29* (22), 1606042.
(43) Monroe, C.; Newman, J. *J. Electrochem. Soc.* **2005**, *152* (2), A396−A404.
(44) Khurana, R.; Schaefer, J. L.; Archer, L. A.; Coates, G. W. *J. Am. Chem. Soc.* **2014**, *136* (20), 7395−7402.
(45) Tikekar, M. D.; Archer, L. A.; Koch, D. L. *Science advances* **2016**, *2* (7), e1600320.
(46) Qiu, Y.; Weng, G. *Int. J. Eng. Sci.* **1990**, *28* (11), 1121−1137.

DOI: 10.1021/acs.nanolett.8b01421
Nano Lett. XXXX, XXX, XXX−XXX

(47) Chen, Y. L.; Wang, S. T.; Liu, B.; Zhang, J. Y. *Composite Structures* **2015**, *122*, 496−506.
(48) Bruce, P. G.; Vincent, C. A. *J. Electroanal. Chem. Interfacial Electrochem.* **1987**, *225* (1−2), 1−17.
(49) Scrosati, B.; Croce, F.; Panero, S. *J. Power Sources* **2001**, *100* (1-2), 93−100.
(50) Wu, M.; Wen, Z.; Liu, Y.; Wang, X.; Huang, L. *J. Power Sources* **2011**, *196* (19), 8091−8097.
(51) Li, N. W.; Shi, Y.; Yin, Y. X.; Zeng, X. X.; Li, J. Y.; Li, C. J.; Wan, L. J.; Wen, R.; Guo, Y. G. *Angew. Chem., Int. Ed.* **2018**, *57* (6), 1505−1509.

DOI: 10.1021/acs.nanolett.8b01421
Nano Lett. XXXX, XXX, XXX−XXX